Monograph:
Moorsom, T (2020) Growth of crystalline C_{60} by evaporation. Report. Materials from the Royce Deposition System (4). University of Leeds

10.48785/100/83

Growth of crystalline C_{60} by evaporation

T. Moorsom

This application note describes the growth of crystalline thin films of C_{60}.

1 Introduction

C_{60}, also known as Buckminsterfullerene, is the most common and stable of the fullerenes, comprising a near spherical cage of sixty carbon atoms. C_{60} has a wide range of applications in molecular electronics and spintronics, solar cells and molecular magnetism. [1–3] The growth of high quality, crystalline C_{60} films is vital for the production of hybrid meta-materials and devices. In this note, we outline the optimal growth parameters for the evaporation of highly crystalline C_{60} films from an effusion cell onto Pt substrates.

2 Growth

C_{60} can be grown easily on various metallic and semi-conducting substrates. C_{60} grows poorly on oxides due to high surface tension, causing large clusters to form. [4] Epitaxial platinum with a (111) texture is an ideal metallic substrate for C_{60} growth. Pt (111) films were grown on Al_2O_3 substrates (see application note for e-beam Pt growth). The substrate temperature was maintained at 20° C. C_{60} was evaporated from a graphite crucible in a single filament effusion cell. The effusion cell temperature was increased from standby at a rate of 10 °C per minute to 430 °C. The deposition rate was measured to be 0.5 Å/s using a quartz balance. The rate varies during growth, reaching a maximum value of 0.74 Å/s. The substrate was rotated at 90°/s during deposition. the background pressure was 8×10^{-10} mbar. After growth, the film was capped with a 15 nm thick film of Nb to protect it from oxidation.

3 Properties

Structural characterisation was obtained using X-ray reflectivity (XRR) and TEM. Figure 1 shows the XRR data taken of the bilayer film. C_{60} has a very low density of 1.65 g/cc. However, a structural peak is observable at 11°. Because of the low scattering length of C_{60}, this peak is only visible in samples with extremely high crystallinity. A GenX reflectivity fit was performed for this data. The low angle fit does not capture the structural peak as this method does not simulate crystal structure.

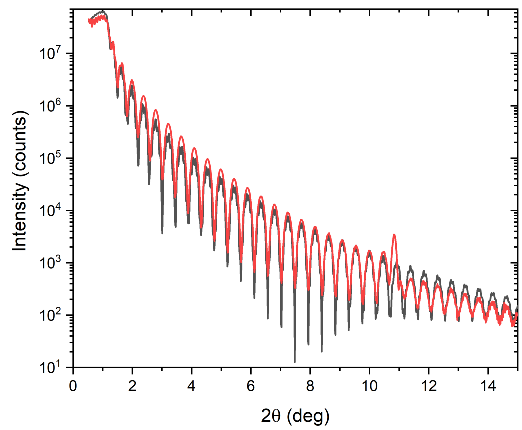

Figure 1: X-ray reflectivity data of a platinum C_{60} bilayer (red) and GenX fit (black). The structural C_{60} peak at 11° is not captured by the low angle fit.

A lamella, 80±10 Å thick, was cut from the sample using a Dual-Beam Ga Ion FIB. This lamella was then measured using a Titan FEI TEM at 100 kV 2. The van der Waals lattice of the C_{60} is clearly visible with (111) vertical orientation. The interface between the Pt and C_{60} is atomically sharp. The lattice spacing of the C_{60} film is 1.05±0.03 nm.

The vibrational spectrum of C_{60} films was recorded

GenX fitting parameter	Value
Thickness - C_{60} (Å)	975±0.7
Density - C_{60} (% of bulk)	100±0.01
RMS Roughness - C_{60} (Å)	1.8±0.9
Thickness - Pt (Å)	191±0.2
Density - Pt (% of bulk)	100±0.01
RMS Roughness - Pt (Å)	1.7±0.1

Table 1: Structural parameters obtained through the fitting of XRR data with GenX

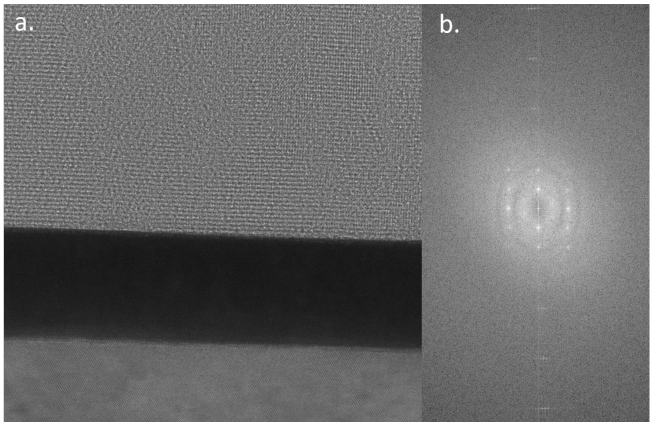

Figure 2: a. TEM obtained from the Pt/C60 bilayer lamella, showing clear molecular layers and an atomically sharp interface. b. FFT of the C_{60} layer, showing 3D crystal structure.

Mode	Raman Shift
Ag(2) - Δcm^{-1}	1470±2
Hg(7) - Δcm^{-1}	1434±5
Hg(8) - Δcm^{-1}	1575±5

Table 2: Positions of the major Raman active modes of C60.

using a Horiba Raman Microscope with a 471 nm diode laser, Figure 3. The three highest intensity Raman active modes: Ag(2), Hg(7) and Hg(8) are used to determine the quality of the film. [5]

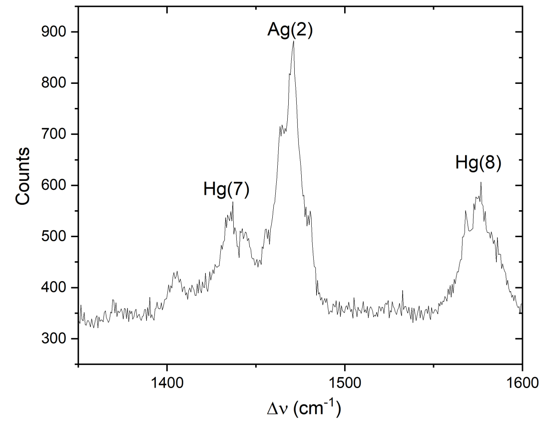

Figure 3: Raman spectrum of C_{60} film. The three major Raman active modes are present and the characteristic mode of graphite at 1600 cm^{-1} is absent. The splitting of the Ag(2) peak is characteristic of electron transfer across a metallic interface.

References

1. W. Kratschmer *et al.*, *Nature*, 354–358 (1990).
2. M. Gobbi *et al.*, *Advanced Materials* **23**, 1609–1613, eprint: `https://onlinelibrary.wiley.com/doi/pdf/10.1002/adma.201004672` (2011).
3. F. A. Ma'Mari *et al.*, *Nature* **524**, 69–73 (2015).
4. F. Loske *et al.*, *Nanotechnology* **20**, 065606 (Jan. 2009).
5. V. Schettino *et al.*, *The Journal of Physical Chemistry A* **105**, 11192–11196, eprint: `https://doi.org/10.1021/jp012874t` (2001).